euspen's 23rd International Conference & Exhibition, Copenhagen, DK, June 2023
www.euspen.eu

Optimization of diamond machined gratings for low light scattering and highest diffraction efficiencies

Ralf Steinkopf[1], Peter Weide[1], Marcus Trost[1], Martin Heusinger[1], Dana Tomuta[2], Roman Windpassinger[2], Jan Kinast[1], Stefan Risse[1]

[1] *Fraunhofer Institute for Applied Optics and Precision Engineering IOF*
[2] *ESTEC - European Space Research and Technology Centre*

ralf.steinkopf@iof.fraunhofer.de

Abstract

Optical instruments for earth observation often rely on high performance spectroscopy. One key element in this technology is the dispersing element. Typically used grating designs in Littrow or Offner spectrometers are blazed or binary phase gratings. The diffraction efficiency of these elements is decisive for the radiometric accuracy of the instrument [1].
One highly effective and accurate technology for the manufacturing of optical gratings is diamond machining. It offers the opportunity to manufacture gratings even on curved base geometries. However, this is achieved by using at least three machine-controlled axes, all contributing to fabrication tolerances and thus reducing the accuracy of the grating shape [2]. The accuracy of the grating features is secured by the use of microscopic analysis and white light interferometry. But, besides of the error impact from mistuned geometric features, dispersive elements with their large surface area are susceptible to light scattering that leads to a reduced spectral purity and lower grating efficiencies. Especially diamond machining with two or more simultaneously moving linear or rotating axes is an excellent source for light scattering.
This publication discusses the influence of the manufacturing technology on the grating performance by analysing their optical impact through light scattering measurements. Further, the paper demonstrates the possibility to enhance the performance of diamond-machined gratings by varying process variables as machine parameters or by changing the substrate material. It shows the potential of combining classic feature analysis with light scattering analysis to enhance the optical performance of dispersive elements significantly.

Keywords: diamond machining, diffraction grating, stray light analysis, dispersive element, spectrometer

1. Introduction

Diffraction gratings are one of the most challenging components of innovative spectroscopic instruments in applications such as remote sensing of the Earth or astronomical spectroscopy [3]. To widen the fundamental understanding, how manufacturing affects the performance of diamond-machined gratings, a test setup is chosen that modifies manufacturing parameter, grating geometry, and grating material (see Figure 1). The test gratings (blazed profile with period p=30 µm and depth d=317 nm) are analyzed with emphasis on geometric accuracy, surface roughness, and light scattering. Especially stray light characteristics, analyzed through Angle Resolved Scattering (ARS) measurements, shall be used as benchmark for the quality of the gratings [4,5]. Dark Field Microscopy (DFM) and White Light Interferometry (WLI) are used to qualify and quantify manufacturing errors. The combined results of these measurement technologies are used to identify and optimize unfavorable manufacturing parameters.
The machine setup is based on a 5-axis diamond turning machine. The machining process is performed as ruling process using only linear axes without relying on rotation axes. The tip of the diamond tool is moving in a linear movement, bottom to top, over the surface, repeating this step for step each line of the grating left to right. The tip of the diamond tool is shaping in this process with each line one edge of a blazed grating.

Material	AL6061 AL6061 + NiP	
Geometry	**Periode**	**nominal** 120% 80%
	Amplitude	**nominal** 120% 80%
	Superperiods	Amplitude 120% Periode 120%
Machine Parameter	**Feed direction**	positive negative
	Speed	**nominal** 120% 80%
	Depth of Cut	**nominal** 120 80%

Figure 1 Design of Experiment

2. Microscopic inspection

Microscopic inspection is an effective tool for qualitative analysis, even without retaining accurate numbers as result. To optimize the test structures, they are cut with different machine parameters and analyzed by DFM. Changing only one machine parameter at a time, allows to identify sensitive parameters that can be roughly adjusted then. The fine tuning is realized with more sensitive tools for quantitative analysis.

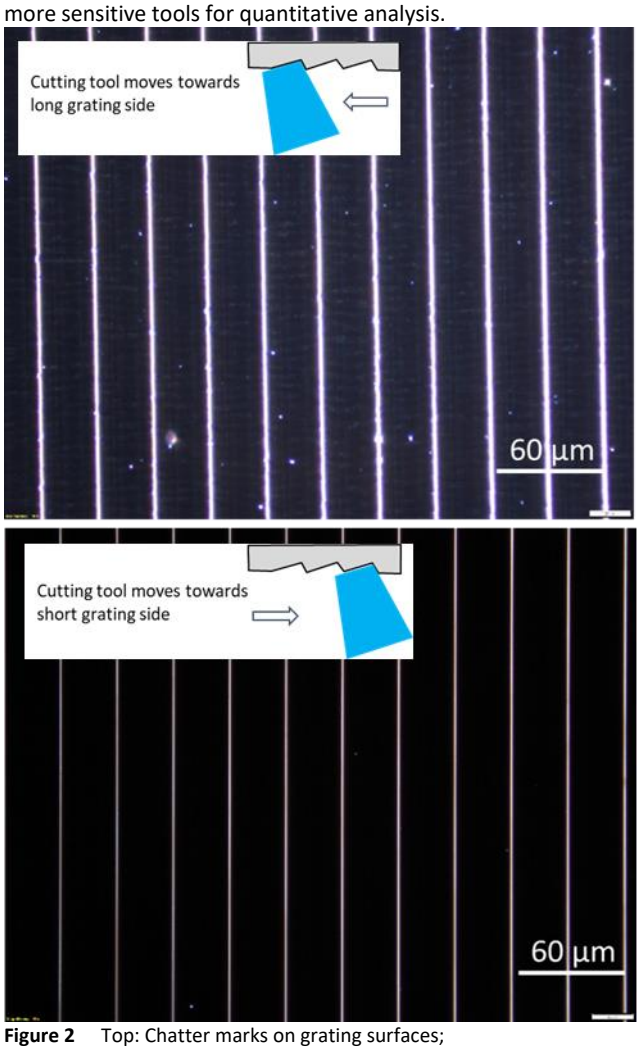

Figure 2 Top: Chatter marks on grating surfaces;
Bottom: Changing the cutting direction reduces chatter marks clearly

Figure 2 shows DFM images of two gratings, machined with different parameter sets. The top picture clearly shows ratter marks within the grating surface (perpendicular to the observable bright tips of the blazed grating) and deformed edges. The bottom picture instead shows straight grating edges and no chatter marks. The decisive parameter in this example is the cutting direction. Each cut of one grating flank results in one small burr at the edge of the flank. By working into the direction of the small flank, the burr is removed with the cut of the next flank as indicated by the small inset schematics on top of the DFM images.

Other machine parameters, as for instance feed rate or cutting depth, result in grating errors too, but they are not as easily to separate and minimize. However, DFM analysis allows for sorting through the parameters, decide about its sensitivity and gives a first impression of the optical performance. Sensitive parameter, that lead to more subtle changes in the grating surface, are optimized by white light interferometry.

3. White Light Interferometry

Grating efficiency depends on accurate grating geometry, namely grating depth and grating width as well as surface parameters represented in micro roughness and waviness. Overall errors resulting from shape deviations of the grating substrate will be ignored in the following, they are not directly connected to the optimization process that is subject of the current study but of course impact the later grating performance.

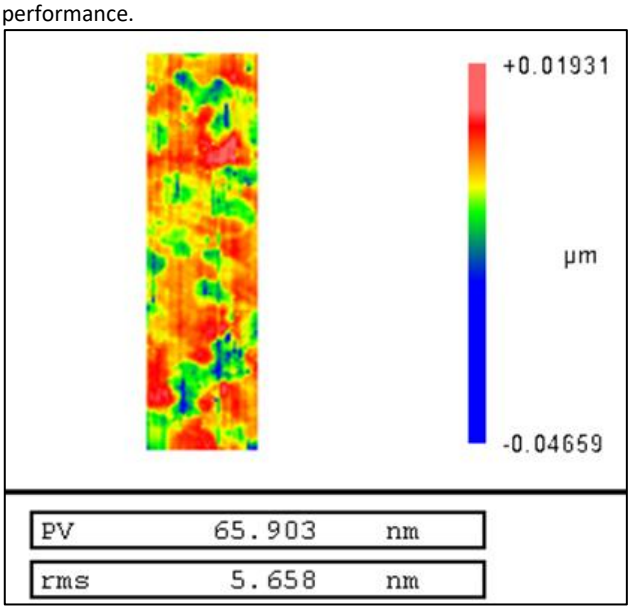

Figure 3 Surface roughness of 6 nm rms (Al6061 substrate)

WLI is an excellent tool for measuring features sizes and quantifying surfaces parameters by calculating microroughness or waviness. This makes WLI a versatile instrument for grating analysis. However, it is not straight forward to conclude from the measured error to the to the impact on optical performance. For this reason, the experimental setup (see Figure 1) consists of deliberately designed errors within the grating, that are analyzed and corrected using WLI and later compared with the results of ARS measurements.

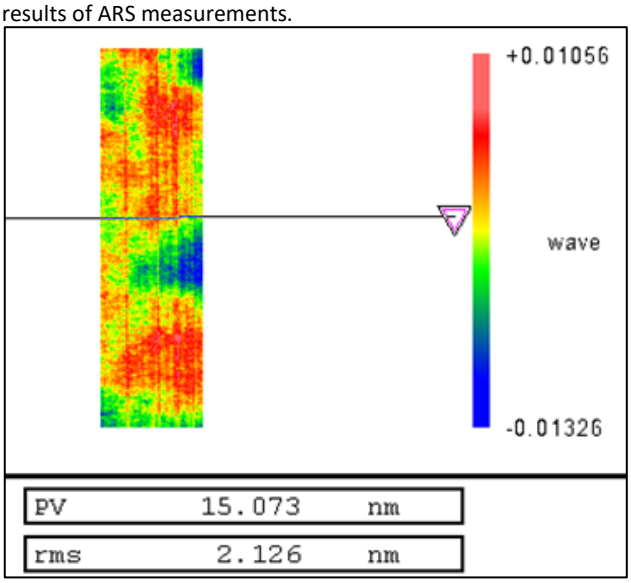

Figure 4 Surface roughness of 2 nm rms (NiP substrate)

One parameter with high impact factor is the substrate material. Figure 3 and Figure 4 demonstrates the surface roughness cutting two different materials, using the same parameter set. Figure 4 shows electroless plated nickel phosphorous (NiP) used as substrate material, with grain structures that are considered as X-ray amorphous. Figure 3 shows Al6061 with considerably larger grain structures. The surface roughness on the grating flanks of the Al6061 test sample is approximately three times as high as the rms roughness of the NiP test sample. Not seen in the picture is the edge deformation that is considerably higher

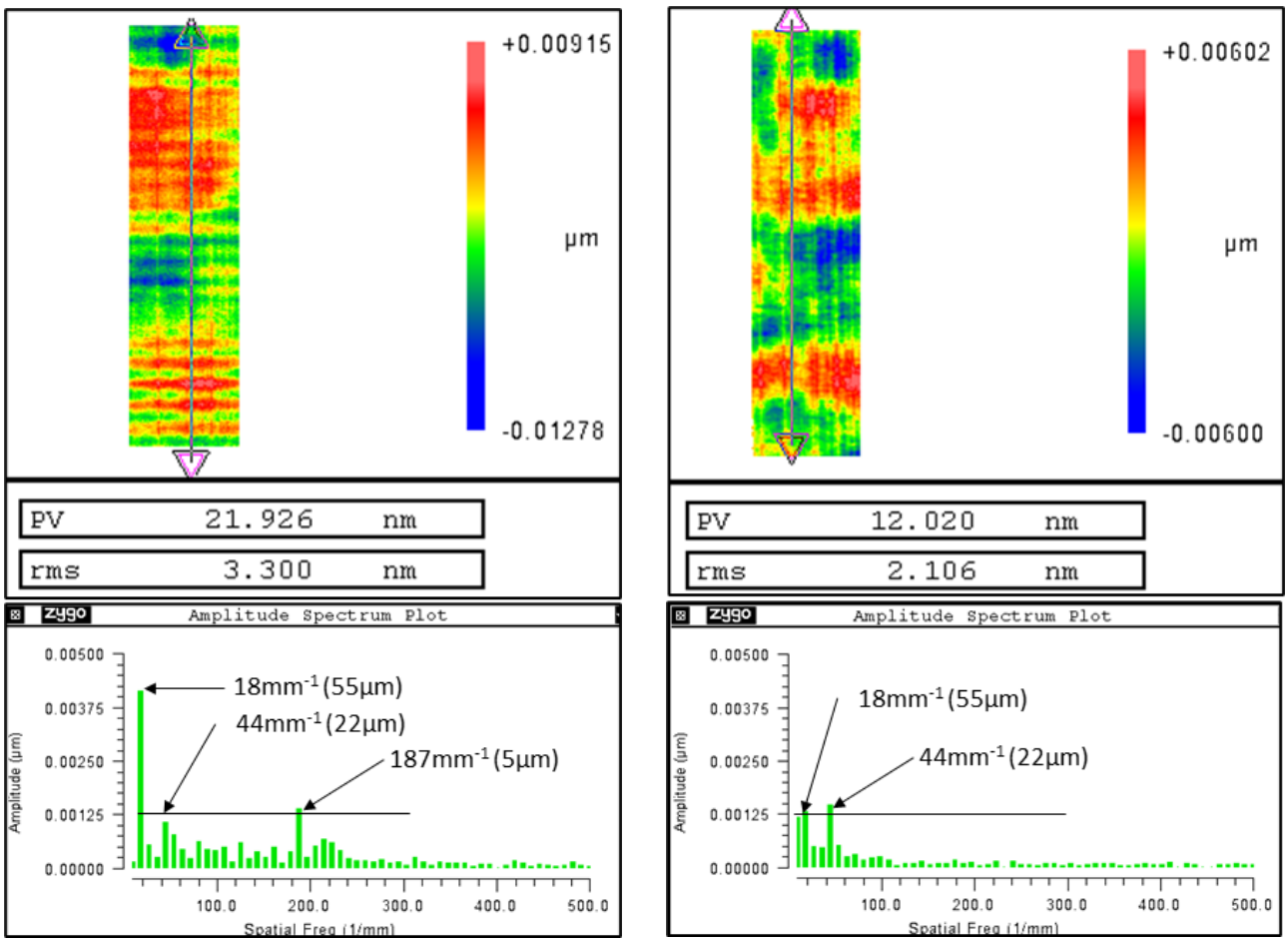

Figure 5 Left side: Surface roughness of 3.3 nm rms and chatter marks in vertical direction, cut with 50 % of nominal speed (NiP substrate)
Right side: Surface roughness of 2.1 nm and no visible ratter marks after enhancing the cutting speed to 200 % of the nominal speed (NiP substrate)

on Al6061, too. Varying machine parameters instead of material parameters result in measurable differences, too. In order to study this in more detail, experience-chosen nominal values (100 %) and two percentage derived values at 80 % and 120 % were used to fabricate sample sets with single varied parameters (see Figure 1). If a parameter set shows a clear direction of improvement in the analysis, additional test parts are cut to find the optimum.

In the example seen on the left side of Figure 5, the feed rate parameter is reduced to 50 % of the nominal feed rate. The surface roughness is 3 nm rms and chatter marks are clearly visible with particularly strong peaks at two spatial frequencies, f=18 mm^{-1} and f=187 mm^{-1}. On the right side of the picture, the feed rate is increased to 200 % of the nominal feed rate. This reduces the surface roughness to 2 nm rms and eliminates the chatter marks effectively. The peak at f=187 mm^{-1} is removed completely and the surface period at f=18 mm^{-1} ranks now unobtrusive within the surrounding topography. To optimize the grating further, the experiment was repeated similarly by varying the cutting depth.

If the machine setup is optimized, the same must be realized for the grating geometry. To substantiate this statement, the study is varying geometry parameters as well as it was described for the variation of the machine parameter. According to the test plan, the period and the amplitude were changed, and super periods were introduced in addition to the grating period (see Figure 1). The adjustments are based on WLI measurements.

Both parameter sets, machine and geometry parameters, are analyzed through ARS measurements, too. In this combination, both parameter sets indicates, how local disturbances on the surface and geometric offsets impact the performance of diffraction gratings

4. Light scattering analysis

ARS measurements were performed with the scatterometer MLS10, developed at the Fraunhofer IOF. As characterization wavelength were 633 nm and 10.6 µm chosen. The latter is used to separate the regular diffraction peaks more clearly and analyze the scattering within the dispersion plane. The measurements at 633 nm were performed in the entire backward hemisphere in order to study ghost diffraction as well as the cross-dispersion plane.

It is expected to detect stochastic imperfections that lead to a homogenous scattering background as well as periodic effects from manufacturing which cause grating ghosts. Stochastic imperfections are likely scattering effects of surface roughness or edge defects, whereas periodic effects most likely result from geometric offsets or periodic imprints of the manufacturing technology. To answer the question about the cause of imperfections, the ARS measurements are analyzed in the context of the WLI and DFM measurements.

The left side of Figure 6 shows two different hemispherical ARS measurements with its typically circular plot caused by the scan process in azimuthal and horizontal direction. The grating is orientated such that the dispersion plane is parallel to the x-axis, which also defines the azimuthal angle of incidence. The impact of chatter marks observed in the DFM and WLI measurements can thus be observed perpendicular to the x-axis. As the plot shows a projection of the scattered light of the backward hemisphere, this cross-dispersion plane is slightly curved. The ideal plot would be monochrome with single luminous spots along the X-axis for the regular diffraction orders. Noticeable on the left hemispherical ARS plot is a large bright spot instead, outshining it surroundings. Obviously, cutting in the direction of

the short side induces a large scattering background. Cutting instead to the long side of the grating (see right hemispherical ARS plot of Figure 6) results in much lower scattering and reveals some luminous spots in the cross-dispersion plane, which might be the result of mechanical induced vibrations during manufacturing.

Measuring with λ = 633 nm does not allow for a detailed analysis within the diffraction plane because the rather large grating period of 30 µm leads to an angular separation of less than 2° between the regular diffraction orders. For a better separation, in-plane ARS measurements were performed at λ = 10.6 µm as shown in the right side of Figure 6. To focus onto the diffraction plane, the measurement is performed in horizontal direction only. The larger wavelength allows "zooming" into the space between the diffraction orders. Obviously, the cutting direction

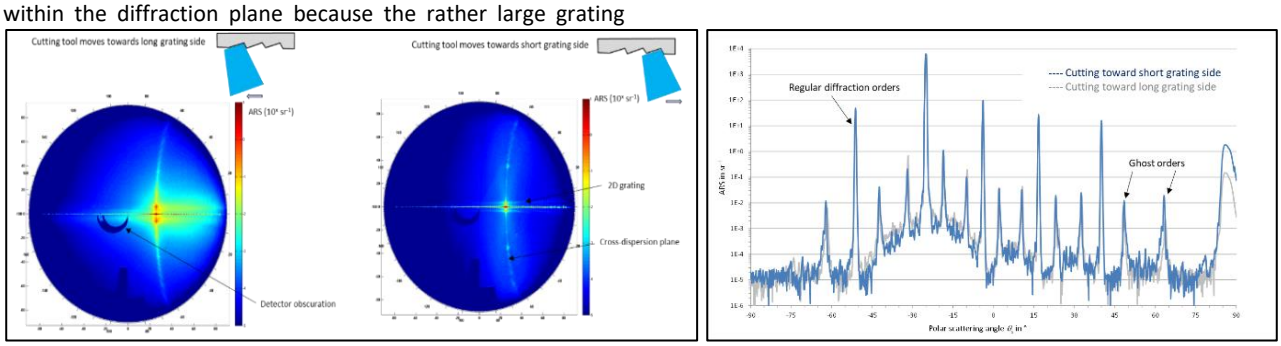

Figure 6 Different ARS measurements of the blazed grating with period p=30µm on NiP substrates
Left side: Hemispherical ARS measurement; Cutting towards the short grating side reduces the scattering around the use order of the blazed grating but pronounces underlying periodic imperfection (Measurement parameters: λ = 633 nm, s-polarized, AOI = 25°)
Right side: ARS measurement within diffraction plane at λ = 10.6 µm for a "better separation" between regular diffraction orders indicating low impact on ghost orders from the cutting direction

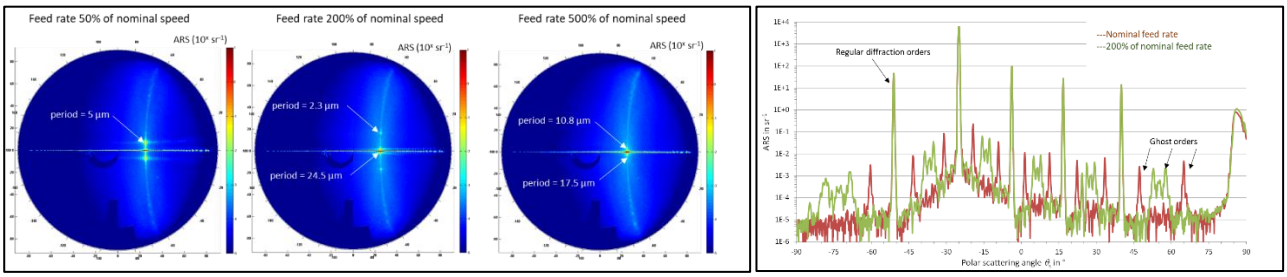

Figure 7 Different straylight measurements of the blazed grating with period p=30µm on NiP substrates: (Left side) Changing machine parameters as feed rate can reduce periodic imperfections or move them in the desired diffraction order (Measurement parameters: λ = 633 nm, s-polarized, AOI = 25°); (Right side) ARS measurement within diffraction plane at λ = 10.6 µm for "better separation" between regular diffraction orders shows how ghost orders can be directed away from the regular diffraction orders by changing machine parameters as feed rate

has just a low impact on the amplitude and on the frequency of the ghost periods. But even so, the ghost orders directly next to the main diffraction order at 25° and the ground noise appear slightly higher for the more unfavorable cutting direction.

As shown in the previous chapter, machine parameters have a high impact onto the waviness within the grating flanks. A further examination of the behavior by ARS measurements is given in Figure 7. The revealed ghost periods are in line with the periods determined by WLI. Interestingly, it is possible to shift the position of the ghost peaks in the diffraction plane away from the regular diffraction peaks. This way, they can easily be blocked by the aperture slit in a spectrometer. Knowing the design of the instrument and the machine imprint, it is possible to shift interfering scattering light spots out of the clear aperture or even onto the main diffraction order to increase the spectral purity of the spectrometer. Zooming into the diffraction plane using λ = 10.6 nm as a characterization wavelength (right side of Figure 7), reveals that changed machine parameters can influence ghost orders in the diffraction plane, too. By changing the feed rate from nominal speed (100 %) to 200 %, the ghost orders are shifted away from the regular diffraction orders, giving a cleaner spectrum at the desired use order of the grating.

5. Conclusion

The combination of DFM, WLI, and ARS measurements allows for a comprehensive analysis of the imperfections of diamond-machined diffraction gratings. It is shown that combined analyzing techniques give insight into manufacturing behavior and its impact on the application side and thus, allowing for an effective correction of stochastic imperfections as well as periodic errors. The most pronounced scattering and ghost diffraction orders are found in the cross dispersion plane and are induced by chatter marks intrinsic to the chosen manufacturing technology. By optimizing machine and material parameters, these ghost orders and the background scattering can be minimized. It is even possible to shift the angular position of the ghost orders away from the regular orders with only marginal impact for the chattering background. This can be used to further optimize a grating for a given spectrometer design.

Acknowledgement

This work was founded by the European Space Agency and European Space Research and Technology Centre under contract no. 40000133909/21/NL/AR

References

[1] De Clercq, et al, "ELOIS: an innovative spectrometer design using a free-form grating", Proc. of SPIE Vol. 9626 96261O-1

[2] R. Steinkopf, et al, "Metal mirrors with excellent figure and roughness", Proc. of SPIE 7102, 71020C1–71020C12, (2008)

[3] Peschel, et al. "Integration and testing of an imaging spectrometer for earth observation" ICSO 2018, Proc. Of SPIE Vol.11180

[4] M. Heusinger, et al, "Light scattering from diffraction gratings", presented at ICSO2022, Dubrovnik (Croatia)

[5] M. Trost et al, "Roughness and Scatter in Optical Coatings," in Optical Characterization of Thin Solid Films, O. Stenzel and M. Ohlídal, eds. (Springer, 2018), pp. 377–405.